

Self-sufficient Method for Event Localization and Characterization of Power Transmission Lines Based on Traveling Waves

Marko Hudomalj, Andrej Trost, *Member, IEEE*, Andrej Čampa

Abstract—We propose a self-sufficient online method that simultaneously performs transmission line characterization and event localization. Our proposed method eliminates the need for offline transmission line characterization or line parameter modeling based on the transmission line model. The method is based on traveling wave theory and adding a measurement device in a double-sided traveling wave event localization setup. The theoretical background of the method is derived, which is based on a complex continuous wavelet transform. The accuracy of the transmission line characterization method is evaluated using a frequency-dependent transmission line simulation model. The method was developed independently of the type of event and is evaluated in a variety of experimental setups that take into account different lengths of the monitored line section, line characteristics, location of the third measurement device, and location of the event. The localization accuracy is compared with other proposed online methods. The proposed method improves event localization and exhibits high characterization accuracy within a relative error of 1%, even when mimicking real environmental conditions where noise and desynchronization between measurement devices occur.

Index Terms—Event localization, propagation characteristic, transmission line, traveling wave, wavelet transform.

I. INTRODUCTION

With the development of smart grids and the increasing complexity of electrical power systems, the need for more advanced monitoring and decision-making is becoming increasingly important. In addition to established monitoring systems that monitor slowly changing electrical properties, many efforts have been made recently to develop new systems that detect and respond to fast transient events to improve power system reliability. Today, systems for detecting the fastest transient events in power systems are based on traveling wave (TW) theory [1].

A significant part of the electric power systems to be monitored are the transmission lines. The sections of transmission lines are typically long and often inaccessible, so effective automatic monitoring solutions are required. TW theory is a well-established method that has been applied to many different solutions for monitoring events on transmission lines.

This work was partly funded by the Slovenian Research Agency under Grant no. P2-0016, and the European Commission through the H2020 project BD4NRG (Grant no. 872613) and Horizon Europe project ENERSHARE (Grant no. 101069831).

M. Hudomalj and A. Čampa are with Jožef Stefan Institute, Ljubljana, Slovenia and with Comsensus d.o.o., Dob, Slovenia (e-mail: marko.hudomalj@ijs.si, andrej.campa@comsensus.eu).

A. Trost is with University of Ljubljana, Faculty of Electrical Engineering, Ljubljana, Slovenia (e-mail: andrej.trost@fe.uni-lj.si).

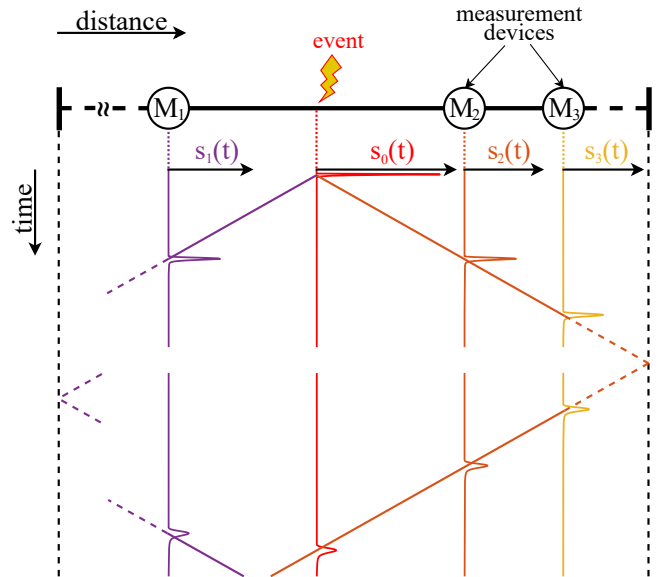


Fig. 1. Lattice diagram of TW propagation on a transmission line in the proposed measurement setup. TW signals are shown over the lattice diagram at the event location and the locations of measurement devices.

Several solutions have been developed that use TW for fault protection and localization [2], lightning strike detection [3], and partial discharge localization and monitoring [4], [5].

An event on transmission line results in a transient signal that propagates along the line away from the location of the event. At the line ends, terminations, or transitions between different types of transmission lines, where the electromagnetic characteristic of the medium changes, part of the wave is reflected while the other part of the wave propagates into the next medium. Due to the frequency-dependent properties of the medium, the waves are attenuated and dispersed. Attenuation reduces the wave amplitude and dispersion elongates the wave in time because the different frequency components propagate with different velocities. A schematic overview of a transmission line with an event that triggers a TW signal is shown in Fig. 1. The signal propagation is visualized with the lattice diagram, over which detailed waveforms are shown at the event location and at the measurement locations. The left and right TW are depicted with the reflections occurring at the end of the transmission line.

In the literature, TW solutions are applied to each specific event type separately, but in this paper we propose a general method for event localization. There are two main approaches for localizing events on transmission lines based on TWs [2]. The first approach is single-sided setup [5], [6] and the second approach is double-sided setup [7], [8]. The single-sided setup uses one measurement device at one end of the line. In Fig. 1, only one measurement device M_1 or M_2 would be used. In this setup, the event location is determined based on the incident and reflected waves and the known propagation characteristic of the line. The second approach requires two measurement devices at each end of the monitored line section and the known propagation characteristic of the line. In Fig. 1, the M_1 and M_3 devices would be used for the second setup. In this case, both devices capture the incident waves, which are used for event localization. As described in the literature, the use of a double-sided setup for event localization improves the accuracy, but the drawbacks are the high requirements for time synchronization between the devices [9]. On the other hand, the use of reflected waves requires high measurement resolution and is problematic under noisy conditions because the reflected waves are further attenuated by reflection between two similar media [10].

Another suggested device setup is the use of multiple measurement devices. It can be deployed on a single line section [11], but most of them have been developed for special cases of hybrid transmission lines [12] and for branched transmission line networks where the measurement devices are placed at the ends of the branches [13], [14].

Most event localization techniques are based on the time measurements of the propagating signal. In general, two timestamps are required for event localization [15]. In this method, the monitored line section length and TW propagation velocity must be known for the calculation. To avoid problems with timestamp accuracy, the authors in [5] proposed a single-sided method based on the cross-correlation between the incident and reflected waves, which also requires the propagation characteristic. In these methods, the propagation characteristic can be calculated based on a transmission line model using the line parameters: the geometry, the conductor properties, and the soil resistance [8]. However, it has been reported that more accurate localization can be achieved by using a measured propagation characteristic [16]. Measurements can be made during line deployment or maintenance, which typically requires that the transmission line is de-energized, which can be problematic when lines are already in service.

Even with measured propagation characteristic, significant errors in localization can occur because the medium changes depending on the environment and the operating state of the line [17]. For overhead power lines, the propagation characteristic changes due to the changing ground resistance, which is affected by the presence of water in the ground and temperature variations [18]. For power cables, on the other hand, the most important factor is dynamic loading, which causes temperature changes in the cable [19].

To alleviate these problems, new solutions for online monitoring have been proposed. Some use a signal generator to periodically produce a transient reference signal on the

transmission line that is detected by the measurement devices to update the propagation characteristic of the line. For example, in [11], the authors use a reference signal generator to determine the propagation characteristic, which is then used to calculate the event location. Similarly, in [6], the authors used a generator to determine the line response before and after a fault on the line. The difference in response is then used to locate the fault. The disadvantage of using a reference signal generator is that additional equipment must be installed on the energised lines and it is only suitable for detecting certain types of events.

For this case, recent works have proposed online methods that do not require propagation characteristic as an input parameter for event localization calculation and do not require reference signal generator. One of these proposed methods combines single- and double-sided setups for online partial discharge localization [9]. The authors used two devices, one at each end of the line. The devices operate as single-sided event localization devices with initial assumption of the propagation characteristic of the transmission line (propagation velocity). After both devices localize an event, its location is refined in iteration steps, where localization result should match from both ends. However, the proposed method requires the detection of reflected waves, which is applicable only for shorter lines and only for a few types of events.

In this paper, we propose a self-sufficient online method for event localization and characterization of transmission lines. This is achieved by using a third measurement device in a double-sided measurement setup. The method combines the steps for event localization and line propagation characterization. Apart from the line lengths, no other parameters are required for the operation of the method. The environmental conditions causing changes in the line characteristic do not affect the localization accuracy. The method is also developed independently of the event type and the use case of the application. Online characterization of transmission lines can be further exploited to provide additional information for monitoring of power systems.

The theoretical basis of the method is derived in Section II. Then, the method is tested in a simulation setup described in Section III-A, and the implementation of the method is described in Section III-B. Then, the results are presented and discussed in Section IV, including a comparison with other methods in the literature. Finally, conclusions are drawn in Section V.

II. THEORETICAL BACKGROUND

In this section, we derive the analytical formulation of our method for event localization and transmission line characterization. Our proposed approach for event localization and transmission line characterization is based on detected TWs that are the result of an event on the line. In this paper, we present the method based on incident TWs. This is done for simplicity and clarity, but the method could also be extended with reflected waves. When using reflected waves, fewer measurement devices could be used, but the disadvantage would be that reflected waves are harder to detect because of the additional attenuation caused by the reflection.

Let us first consider the well-known forward TW propagation on a transmission line, as shown in Fig. 1, traveling from the location of the event to measurement device M_1 . The signal of the event at the origin in the time domain in Fig. 1 is s_0 and the signal at the measurement device M_1 at distance x from the event source location is s_1 . In the frequency domain, they are related as:

$$\hat{s}_1(f) = e^{-x\gamma(f)}\hat{s}_0(f) \quad (1)$$

where \hat{s}_0 is the Fourier transform of the event signal s_0 and \hat{s}_1 is the Fourier transform of the signal at distance x from the event origin. Transmission line is parametrised by complex and frequency dependent propagation constant γ :

$$\gamma(f) = \alpha(f) + i\beta(f) \quad (2)$$

where α and β are frequency dependent real and imaginary parts of the propagation constant representing attenuation and dispersion, respectively. Additionally, γ can be normalised for better representation, which gives the complex refractive index:

$$n(f) = \gamma(f)\frac{c}{2\pi f} \quad (3)$$

where c is the speed of light.

Phase constant defines the wave propagation velocity at which the wave travels along the line. Ideal sine wave on the line would propagate with so called phase velocity:

$$v_p(f) = \frac{2\pi f}{\beta(f)} \quad (4)$$

The envelope of a signal consisting of multiple frequency components travels with the group velocity, which is related to the change of propagation constant:

$$v_g(f) = \frac{2\pi}{\beta'(f)} \quad (5)$$

Characterization of transmission lines can be based on time-frequency signal analysis. In our approach, we use the wavelet transform to transform the measured time-series samples into time-frequency space. We used wavelet transform because it has good time and frequency resolution, which is necessary for transient signal analysis [2]. The event is localized based on the line characterization and the computation is performed in the same step. In this paper, we describe a method where three measurement devices are positioned along an observed line dividing the line into two sections. The distances between the measurement devices must be known. With this configuration of measurement devices, a section without an event can always be selected. A diagram of an observed transmission line section with three measurement devices is shown in Fig. 2.

Measurement devices are marked M_1 , M_2 and M_3 and the event location on the line is marked with a lightning bolt. The diagram shows the observed line segment between measurement devices M_1 and M_3 . The line can extend beyond the devices as indicated by the dashed lines. Depending on how far the line extends beyond these two measurement devices, the time of the reflections and their magnitude change. As mentioned earlier, in this derivation we consider only the

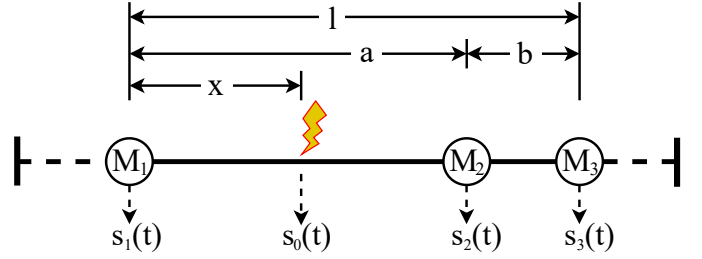


Fig. 2. Diagram of a transmission line in the proposed 3-measurement devices setup with marked distances and considered time-series signals.

incident waves. The signals at the measurement locations are denoted by s_1 to s_3 , while s_0 is the signal at the event location.

The distances between the measurement devices are known. We set the reference position at the location of measurement device M_1 . The length of the whole observed line section up to the device M_3 is l . The unknown location of the event is marked with x and the distance to the device M_2 is marked with a . The length between devices M_2 and M_3 is marked with b , which is also known.

The equations describing the signal propagation along the transmission line to the measurement devices, as marked in the diagram in Fig. 2, can be summarised as:

$$\begin{aligned} \hat{s}_1(f) &= e^{-x(\alpha(f)+i\beta(f))}\hat{s}_0(f) \\ \hat{s}_2(f) &= e^{-(a-x)(\alpha(f)+i\beta(f))}\hat{s}_0(f) \\ \hat{s}_3(f) &= e^{-(l-x)(\alpha(f)+i\beta(f))}\hat{s}_0(f) \end{aligned} \quad (6)$$

Variables \hat{s}_1 to \hat{s}_3 are the Fourier transforms of the sampled signals at measurement locations and \hat{s}_0 is the Fourier transform of the signal at the event location.

By combining equations for \hat{s}_2 and \hat{s}_3 we get:

$$\hat{s}_3(f) = e^{-(l-a)(\alpha(f)+i\beta(f))}\hat{s}_2(f) \quad (7)$$

where unknown variable of the event location x is eliminated and only known distances remain. If the event is located in line section between M_2 and M_3 similar equation can be derived which relates signals from devices M_1 and M_2 .

Equation (7) can be transformed from the frequency domain to the time-frequency domain using the wavelet transform. The complex Continuous Wavelet Transform (CWT) is used in our method. The derivation of equations and in-depth analysis was done by Kulesh et al. [20]. The transformation from Fourier transform to wavelet transform is done with the approximation of the phase constant β with the first two terms of the Taylor series around f . The resulting equation in the wavelet domain is:

$$\begin{aligned} W_g s_3(t, f) &= \\ &= e^{-(l-a)(\alpha(f)+i(\beta(f)-f\beta'(f)))} W_g s_2\left(t - \frac{(l-a)\beta'(f)}{2\pi}, f\right) \end{aligned} \quad (8)$$

where W denotes the continuous wavelet transform and g denotes mother wavelet. The equation describes that a wave at a specific frequency is delayed, attenuated and phase shifted when passing from the location of the device M_2 to the

location of the device M_3 . If we look at only the magnitude part of the complex values of the wavelet transform we get:

$$|W_g s_3(t, f)| = e^{-(l-a)\alpha(f)} |W_g s_2(t - \frac{(l-a)\beta'(f)}{2\pi}, f)| \quad (9)$$

We chose the maximums of the wavelet magnitude at different measurement positions as specific points on the wave to compare the travel times at each wavelet frequency. The times of the maximum wavelet magnitude at each measurement device can be written as t_{maxi} in:

$$\max(|W_g s_i(t, f)|) = |W_g s_i(t_{maxi}(f), f)| \quad (10)$$

$$i \in 1, 2, 3$$

The maximum point at the location M_2 is delayed and attenuated compared to measurement location M_3 :

$$\begin{aligned} |W_g s_3(t_{max3}(f), f)| &= \\ &= e^{-(l-a)\alpha(f)} |W_g s_2(t_{max3}(f) - \frac{(l-a)\beta'(f)}{2\pi}, f)| = \\ &= e^{-(l-a)\alpha(f)} |W_g s_2(t_{max2}(f), f)| \end{aligned} \quad (11)$$

By comparing the delay part of (11) we get:

$$t_{max2}(f) = t_{max3}(f) - \frac{(l-a)\beta'(f)}{2\pi} \quad (12)$$

The time difference of the travel times between the device locations can be expressed as:

$$\Delta t_{max23}(f) = t_{max3}(f) - t_{max2}(f) \quad (13)$$

Group velocity can be expressed from (12) by considering (5) and the time difference (13). The resulting equation is:

$$v_g(f) = \frac{l-a}{\Delta t_{max23}(f)} \quad (14)$$

where we get a known result that the time difference of two points on the wave envelope, in our case the magnitude peak values at each wavelet central frequency, travel with the group velocity.

Attenuation constant can be calculated from (11) and expressed as:

$$\alpha(f) = \frac{\ln\left(\frac{|W_g s_2(t_{max2}(f), f)|}{|W_g s_3(t_{max3}(f), f)|}\right)}{l-a} \quad (15)$$

With a similar approach the phase constant can be derived as:

$$\begin{aligned} \beta(f) &= f\beta'(f) + \\ &+ \frac{\arg(W_g s_2(t_{max2}(f), f)) - \arg(W_g s_3(t_{max3}(f), f))}{l-a} \end{aligned} \quad (16)$$

where β' is correlated with v_g by (5).

From the phase constant the phase velocity can also be determined with (4).

The location of the event can be calculated by combining \hat{s}_1 and \hat{s}_2 from (6). With the transformation in wavelet transform we get:

$$\begin{aligned} W_g s_3(t, f) &= \\ &= e^{-(l-2x)(\alpha(f)+i(\beta(f)-f\beta'(f)))} W_g s_1\left(t - \frac{(l-2x)\beta'(f)}{2\pi}, f\right) \end{aligned} \quad (17)$$

From this equation the event location can be determined from the delay part with a known β' . The location is expressed as:

$$x(f) = \frac{l}{2} - \frac{\pi(t_{max1}(f) - t_{max2}(f))}{\beta'(f)} \quad (18)$$

The described derivation of attenuation and phase constant that define the propagation characteristic and the event location is the basis for our self-sufficient method. The method was implemented and evaluated with the use of simulation which is described in the next section.

III. METHODS

This section is divided in two subsections. Subsection III-A provides the information about the simulation setup used. The results of the simulation are generated time-series signals that would occur on the line at the measurement points. The time-series signals were then input into the proposed method, which implementation is described in Subsection III-B.

A. Transmission line simulation

The evaluation of the proposed method was performed using the results of a simulation of a transmission line on which TW was induced. The output of the simulation are sampled values at the measurement devices locations M_1 to M_3 . The sampled values are input to the proposed method, which is implemented based on the theory from the previous section.

The simulations were performed in different experimental setups where the parameters of the simulation were changed. In the experiments, the parameters l , a , and x were varied. In addition, different transmission line parameters, event types, different noise levels of the sampled signals, and desynchronization between the sampled values were considered.

The simulation environment used for the simulation was Matlab Simulink. A frequency-dependent transmission line model [21] was used to simulate TWs on transmission lines. The model is an implementation of the universal line model which uses frequency-dependent resistance, inductance, and capacitance (RLC) parameters per metre of length. The frequency-dependent model is suitable for simulating transient signal behaviour on transmission lines [22]. We used the model to simulate a transmission line with a single conductor. To simulate different line parameters, we changed the RLC parameters of the simulation with which we modelled overhead and underground transmission lines.

Five transmission line models were used to model the measurement setup from Fig. 2. The simulation model diagram is shown in Fig. 3. The models connected in series divided the simulated line into several sections. To simulate the measurement devices, voltage measurements were taken at each junction between two transmission line models. In reality, the samples between the measurement devices are not fully aligned in time, which is not the case in the simulation. For this reason, additional tests were performed in which the measurement devices were desynchronized. Events were generated using a current generator between the second and third transmission line models. To simulate a homogeneous transmission line where the medium does not change along

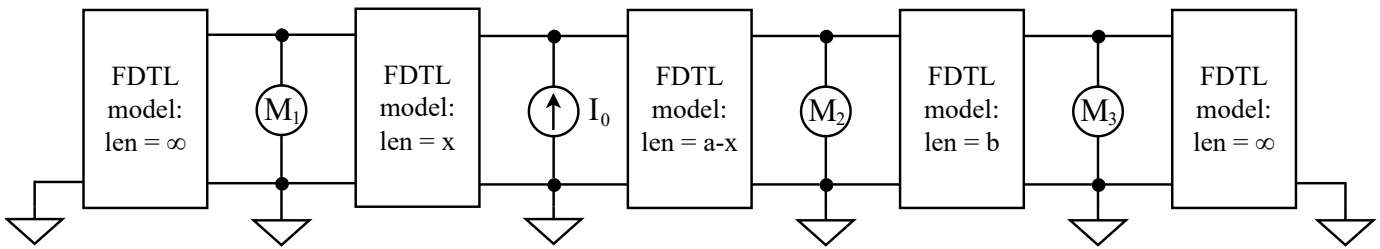


Fig. 3. Diagram of the used transmission line simulation model in Matlab Simulink. Five frequency dependent transmission line models (FDTL model) are used with voltage measurements M_1 to M_3 in between and a current source I_0 for event waveform generation.

TABLE I
USED LINE PARAMETERS FOR THE FREQUENCY-DEPENDENT LINE MODEL.

	Parameter	Value
Underground cable [9]	Below ground	2 m
	Cable core radius	28.25 mm
	Cable core resistivity	$1.75 \cdot 10^{-8} \Omega \text{ m}$
	Internal insulation radius	47.5 mm
	Metal shield radius	50.9 mm
	Shield resistivity	$2.8 \cdot 10^{-7} \Omega \text{ m}$
	External insulation radius	55.9 mm
	Relative insulation permittivity	2.3
	Earth resistivity	100 $\Omega \text{ m}$
Overhead line	Height	16 m
	Conductor outer diameter	2.5 cm
	Conductor thickness/diameter ratio	0.5
	Conductor resistivity	$2.65 \cdot 10^{-8} \Omega \text{ m}$
	Conductor relative permeability	1
	Included skin effect	yes
	Earth resistivity	100 $\Omega \text{ m}$

the wave propagation path, all connected models had the same line parameters except for the line lengths. The line lengths were varied, which allowed us to perform experiments with different parameters l , a , and x . In this work, we focused on the incident waves, so the first and fifth line sections were set to long lengths to delay the reflections and eliminate them from the simulation results. Because an event on the b section of the line corresponds to that on the a section, where the segment lengths are reversed, only experiments with the event generated on the a section were performed.

As mentioned earlier, each of the transmission line sections models had the same RLC line parameters. The evaluation of the proposed method was performed for different transmission line models with different line parameters: the first one represents an overhead transmission line and the second one an underground cable. The frequency range of the RLC parameters was set from 1 Hz to 10 MHz in a logarithmic scale of 1000 points, which enables accurate simulation of transient signal propagation in a wide frequency range. The line parameters used to generate the RLC parameters are gathered in the Table I.

The line was simulated with no operating voltage applied because only the transient behaviour was of interest. Two types of events were simulated. The events simulated were partial discharges and lightning strikes. The partial discharge was modelled with a sum of Gaussian waveforms as described by

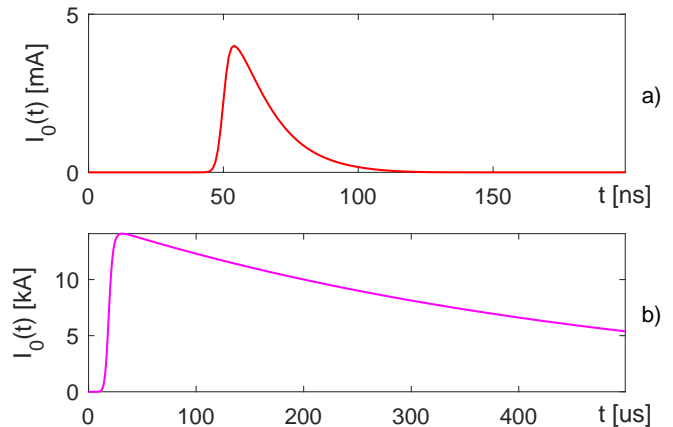


Fig. 4. Waveforms used to simulate the different event types: a) partial discharge and b) lightning strike.

the authors in [23], while the lightning strike was modelled with Hiedler's model presented in [24]. The waveforms used are shown in Fig. 4.

The partial discharge simulations ran with a short simulation step of 1 ns, while we used a simulation step of 100 ns for the lightning simulations. The voltage measurements between the transmission line models were performed with a sampling frequency of 100 MHz for the partial discharge simulations, while 10 MHz was used for the lightning strike simulation. The sampling frequencies used are within the range of the proposed sampling frequencies of 1 MHz to 1 GHz used by other authors [5], [9]. The duration of the simulation was adjusted to the different line lengths and the duration of the simulated events.

To evaluate the method under different noise conditions, noise was added to the time samples. A time delay was also added to the time-series samples to simulate time desynchronization between the measurement devices. The time-series sampled values with their timestamps were then the input for the method, which is presented in the next section.

B. Proposed method implementation

The method was implemented in Matlab. The method is represented with a block diagram in Fig. 5. The diagram shows the different calculation steps, labelled I. through V., which are described below. For each step, an instance of the results for one of the experimental cases is given.

The time-series samples from the simulation measured values are input to the proposed method which is labelled as

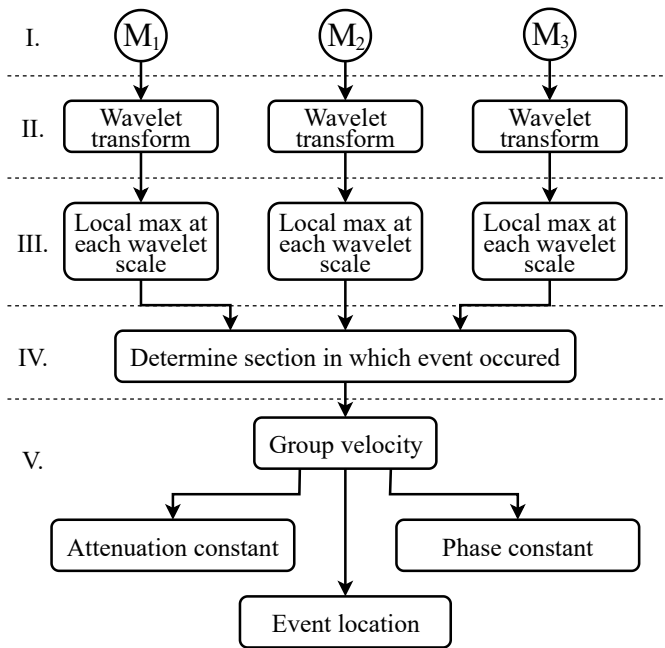


Fig. 5. Block diagram of the proposed method implementation.

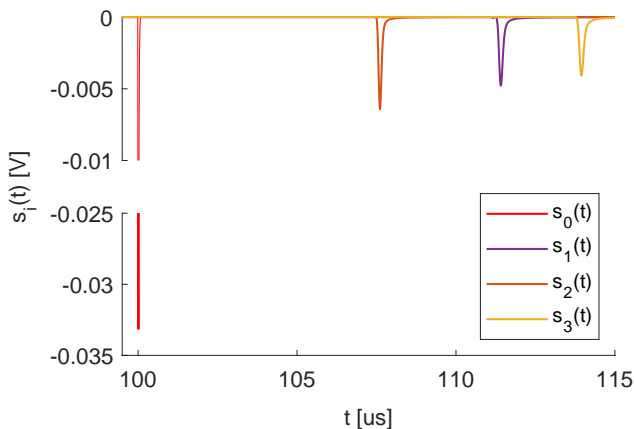


Fig. 6. Measured voltage signals and the triggered partial discharge event on a $l = 5$ km underground cable. The additional measurement device is placed at a distance $b = 1/4l$ and the event is located at a distance $x = 3/5a$. Measured signals are the input to the method in Step I.

Step I. in Fig. 5. An example of the simulation output, which are input for the method, is shown in Fig. 6. In the example partial discharge event was generated on the underground cable with parameters from Table I. The graph in Fig. 6 shows the signal of the event and the measured signals at each measurement location.

Samples are transformed with CWT in Step II. We used a complex Morlet wavelet as the mother wavelet for the CWT [20]. Using the wavelet transform, we obtain a complex time-frequency representation of the signal. In the Step III, a local maximum in time is determined in the time-frequency space of the spectrogram representation of the transformed signal at each wavelet scale with the central frequencies f . The local maximum is also used for event detection in our case, while in practice another event detection algorithm could be used

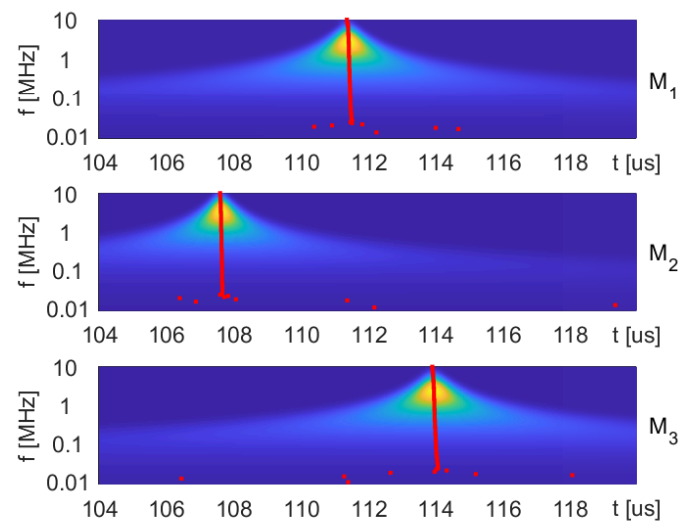


Fig. 7. Spectrograms of the signals at measurement locations using CWT on a $l = 5$ km underground cable with the additional measurement device at a distance $b = 1/4l$ and partial discharge event location at a distance $x = 3/5a$. This is an example of output in Step II. On the spectrograms the local maximums are indicated in red which is the output of Step III.

to reduce computational complexity. An example of Step II and Step III can be found in Fig. 7, where spectrograms for different measurement locations are shown with indicated maximum values at each wavelet scale.

In Step IV, the timestamps of the local maximums are compared to determine on which side of the measurement device M_2 the event originated. This information is used to select the end device of the section where no event was present. By comparing the timestamps of the local maximum at the selected end device and the M_2 device, the group velocity is calculated with (14) in Step V. Based on the group velocity, the event can be localized and characterised. An example of the characterization is shown in Fig. 8. Here, an approximation is made such that the central frequency of each scale represents a single frequency component, as was done in [20]. Since the propagation constant greatly changes with frequency, we used the refractive index to compare the results. The refractive index is proportional to the propagation constant and normalised by frequency (3). The absolute value of the measured refractive index is compared with the input characteristic of the line model. Very good agreement is obtained between the modelled and the calculated refractive index.

After evaluating the implemented method, we performed the sensitivity analysis, where the method steps were used for each tested example.

IV. RESULTS AND DISCUSSION

The proposed method was evaluated in several use cases using the simulation setup presented in Section III-A. The evaluation was performed separately for each of the event types, since the existing TW methods in literature were developed for specific event types. First, we compared the method with the state of the art in event localization, which we present in Section IV-A, and in Section IV-B we present the result where we evaluated the accuracy of our proposed method in

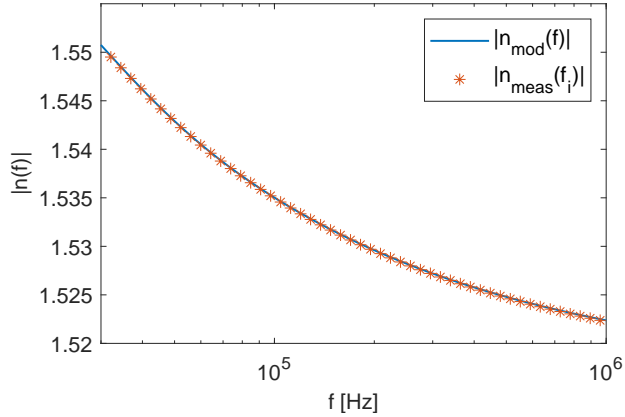


Fig. 8. Absolute value of the measured refractive index profile compared to cable model profile on a $l = 5$ km underground cable with the additional measurement device at a distance $b = 1/4 l$ and event location at a distance $x = 3/5 a$. This is the combined normalised output of the method in Step V.

measuring the propagation characteristic of the transmission line.

In the results reported in this section, we used the frequencies in the range from 30 kHz to 1 MHz for partial discharge experiments and the frequency range from 50 kHz to 200 MHz for lightning strike experiments. The ranges were chosen because the signal cannot be used at higher frequencies in a real measurement setup due to high attenuation, especially on longer lines [11]. At lower frequencies, the wavelength is longer and the size of the sampling window would have to be much larger, which would be impractical in real-world applications.

A. Localization comparison

The proposed method was compared with localization results of existing state of the art online method [9]. Similar to our method, this method is not affected by the changing line parameters during operation. For comparison, we used a partial discharge event. In this case, results were collected on a 1500 m long transmission line where partial discharge signals were triggered at various locations along the line. The transmission line parameters and simulation setup were adapted to those used in [9], and presented in Section III-B. For the results of our proposed method, which requires an additional measurement device, the M_2 device was placed at a distance of $a = 1000$ m as shown in Fig. 2. As will be shown in Section IV-B, the chosen location is not optimal for our method and even better results could be obtained if the M_2 device was placed closer to the middle of the line. For the results of our method, localization was calculated based on the averaged localization results at wavelet central frequencies ranging from 30 kHz to 1 MHz. The results of the compared localization methods are summarised in the Table II. The table contains the real event location x and the localization results for both methods: x_{single} for the improved single-terminal method [9], and the localization results for our proposed method $x_{proposed}$. In addition, the relative localization errors compared to the total observed line length are given.

TABLE II
COMPARISON OF LOCALIZATION ACCURACY OF DIFFERENT LOCALIZATION METHODS FOR PARTIAL DISCHARGE EVENTS.

Single-terminal method [9]		Proposed method		
x [m]	x_{single} [m]	$\frac{ x-x_{single} }{l}$ [%]	$x_{proposed}$ [m]	$\frac{ x-x_{proposed} }{l}$ [%]
200	202.0	0.13	200.3	0.02
300	299.9	0.01	300.2	0.01
400	398.6	0.09	399.7	0.02
500	499.7	0.02	500.0	0.00
600	599.8	0.01	600.2	0.01
700	700.2	0.01	699.9	0.01
750	750.2	0.01	750.0	0.00

Both methods show very good localization results, however our proposed method gives even better localization agreement, which is due to the consideration of dispersion. Even though a real-world application where a partial discharge monitoring system would be used for power cable maintenance and repairs, the localization accuracy of less than 1 m is more than adequate. For longer lines, both methods would suffer, but our proposed method does not use reflections that would be problematic for the compared method. In addition, dispersion has a greater effect on longer lines, which is not accounted for in the compared method, so the results would suffer even more. The problem of dispersion not being taken into account is already evident in the event closest to the end of the line.

To evaluate our method in more detail, we tested it in many different scenarios with a wider range of line lengths and event locations.

B. Method accuracy analysis

In addition to event localization, our method also determines the propagation characteristic of the transmission line. In this section, we present the accuracy of the measurements of the propagation characteristic.

As described in Section II, the transmission line characteristic are completely determined by the propagation constant (2). In this section, we compare the simulation-based measured characteristic obtained with our method to the frequency dependent characteristic of the transmission line model used in the simulation presented in Section III-A. An example of the comparison for a particular evaluation experiment is shown in Fig. 8. To compare the characteristics in a frequency range, the relative errors between the measured and model characteristics at each wavelet central frequency were calculated. The relative errors were calculated with:

$$\gamma_{err}(f_i) = \frac{\sqrt{(\alpha(f_i) - \alpha_{model}(f_i))^2 + (\beta(f_i) - \beta_{model}(f_i))^2}}{\sqrt{\alpha_{model}(f_i)^2 + \beta_{model}(f_i)^2}} \quad (19)$$

$f_i \in CWT \text{ central frequencies}$

where α_{model} and β_{model} are the model attenuation and phase constants and the α and β are the measured attenuation and phase constants.

We present method accuracy results in error plots for different evaluation experiments. The error plots visualize the

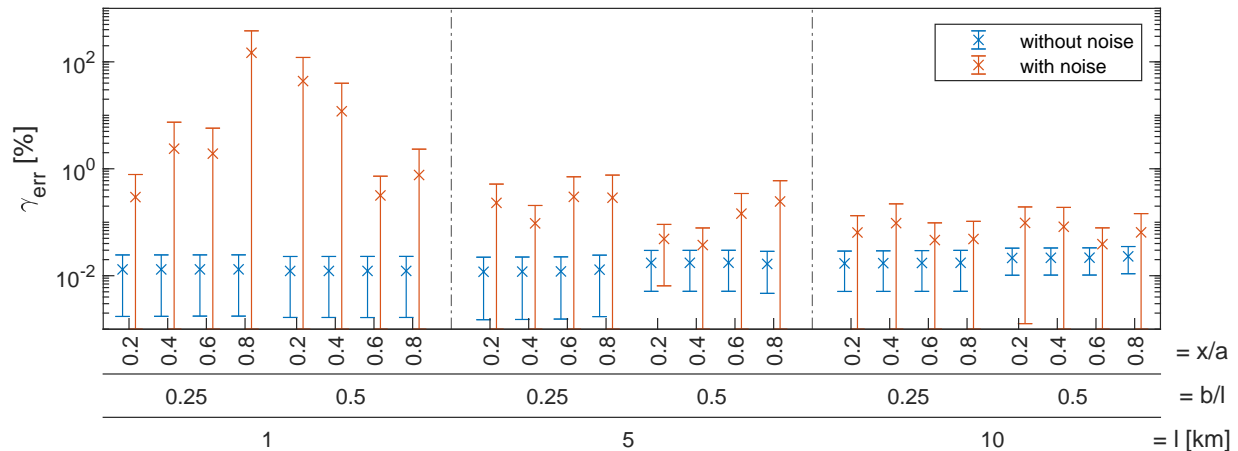


Fig. 9. Propagation constant measurement relative error distribution in the frequency range of 30 kHz to 1 MHz for 1 km, 5 km and 10 km long underground cable with partial discharge event.

distribution of relative error values of the measured characteristic in a range of wavelet central frequencies for an evaluation example. For each example, the average and standard deviation of the relative error values are plotted.

In the first evaluation example, we used the partial discharge event shown in Fig. 4 a). The simulation was performed with the underground cable presented in Table I. The results of the propagation constant accuracy are shown in Fig. 9. The evaluation was performed for different line lengths and event locations on the line. To evaluate the effects of additional measurement device placement along the observed line section, different device locations were considered. The observed cable lengths were 1 km, 5 km, and 10 km. We evaluated the effects of the placement of the device M_2 at two locations: at the middle point and at $b = 1/4l$. The effects of the location of the event were evaluated at 4 points along the line on the a side of the M_2 device. All results were performed under ideal conditions without noise and under noise conditions. Noise was added to the simulation output before it was input to the method. The noise output was set to a signal-to-noise ratio (SNR) of 60 dB compared to the peak value of the triggered event signal. This means that the base noise level was the same for each measurement device, but the TW SNR depended on the location on the line. This means that on longer lines the SNR at the measurement devices was much worse because the TW signal was more attenuated.

The second evaluation example was performed for a lightning strike event as shown in Fig. 4 b) on the overhead transmission line, as presented in Section III-B. Fig. 10 shows the results of the measurement accuracy of the propagation constant for the lightning strike event. In these examples, we used longer line lengths of 10 km, 50 km, and 100 km. As in the case of the partial discharge event, we evaluated the effects of the location of the M_2 device at two locations and the event location at 4 points along the line.

The results show that under ideal conditions the method characterizes the line propagation characteristic with similar results for the entire range of conditions tested. In the ideal

case without noise, the measured propagation constant has an error of about 0.1%. Under noise conditions, the characterization results are within the 1% error range, except for very short lines. For very short lines, the sampling accuracy is not sufficient under noise conditions, which could be improved with higher sampling rates. It should be noted here that the frequency range must be chosen for each of the event types, since the slower changing transient events contain less energy at higher frequencies and the noise degrades the characterization capabilities at higher frequencies. This is also true for the longer lines, where attenuation at higher frequencies in particular limits the capabilities of the method. The lower frequency limit is set by the wavelet resolution used, as it is limited by the sampling time window and the sampling frequency.

One of the specific parameters affecting our method is the location of the measurement device M_2 . From the presented results, it is shown that it does not significantly affect the localization and characterization results. From the error distribution under noise conditions, we can conclude that it is better to position the measuring device M_2 in the middle of the observed line segment. This means that the two devices used for the group velocity calculation have a larger distance b from each other and thus the time difference of the maximum values of CWT is larger and thus less affected by the noise.

In addition, we tested the influence of the accuracy of time synchronization between the measurement devices on the proposed method. The experiments were performed for the case of a partial discharge event, which is the shortest event discussed and therefore requires the highest time accuracy. For this evaluation, a constant time delay was added to the simulation time-series output representing the measurements of the devices. The constant delay was added to represent the absolute time error, since the change in relative time error would not change significantly within the duration of the event. The measurement devices could be synchronized with the Global Positioning System (GPS). The achievable synchronization of the instruments with GPS is 100 ns relative to

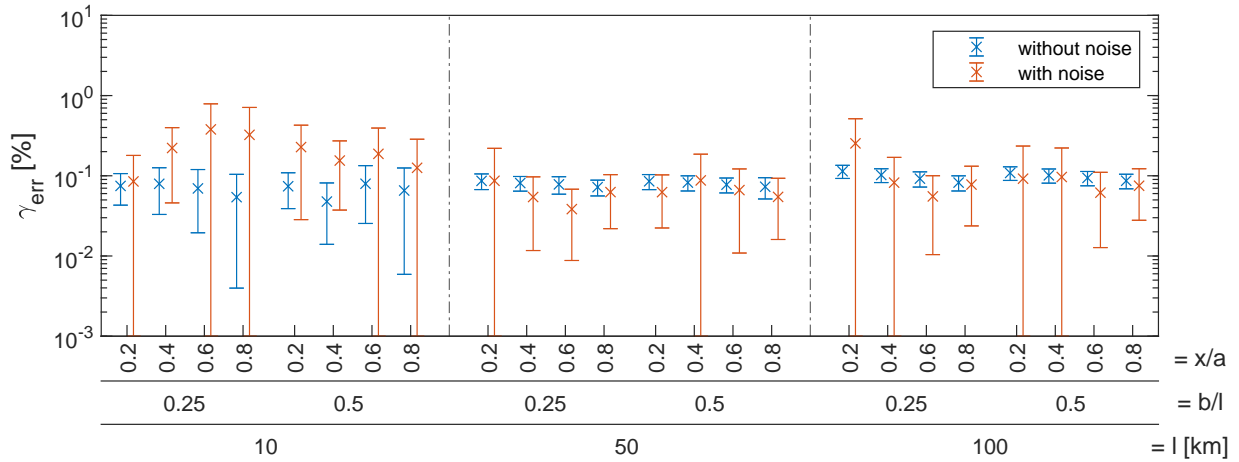


Fig. 10. Propagation constant measurement relative error distribution in the frequency range of 50 kHz to 200 MHz for 10 km, 50 km and 100 km long overhead transmission line with lightning strike event.

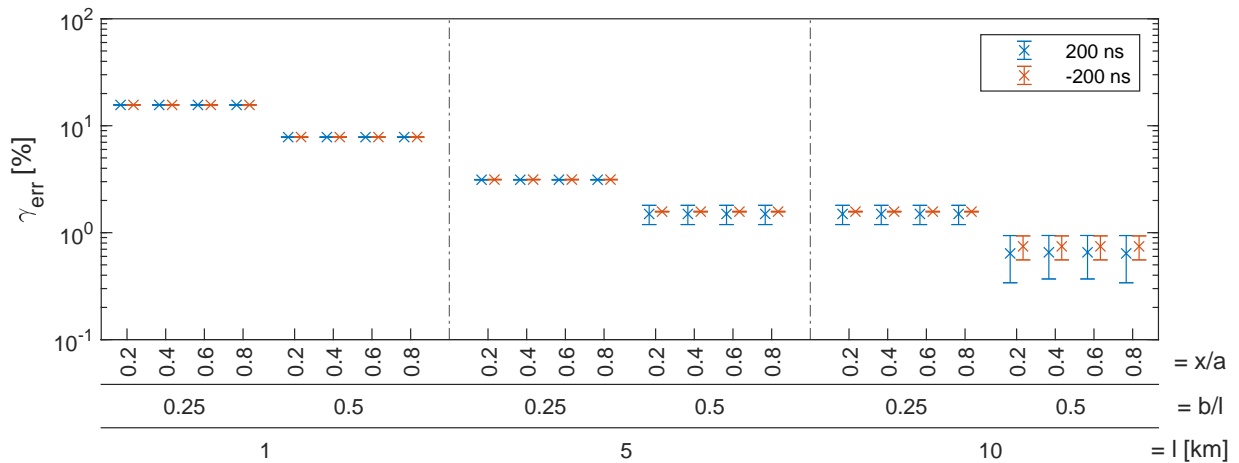


Fig. 11. Propagation constant measurement relative error distribution in the frequency range of 30 kHz to 1 MHz for 1 km, 5 km and 10 km long underground cable with partial discharge event with different desynchronization times between measurement devices.

absolute time [7]. Thus, the worst-case time desynchronization between the middle and edge device can be ± 200 ns, which was used in synchronization accuracy experiments. The results are shown in Fig. 11. The figure shows the relative errors of the transmission line propagation constant measurements for different examples. The sampling time jitter that would occur in the event duration was considered negligible.

The results in Fig. 11 show that for longer distances, where the distance between the middle device and the edge device is also larger, the GPS time synchronization can be used because the time error is much smaller compared to the time it takes for the TW to propagate between two measurement devices and thus does not affect the measurement. In this case, the relative error of the propagation characteristic of 2% can be achieved. On shorter lines, the timing desynchronization has a greater effect because the time the wave travels between the measurement devices is shorter. For this case of shorter line sections, greater timing accuracy is needed, which can be achieved by using optical cables.

In the results presented, we set the simulation to ignore

reflections. If reflections were present in the system, they could be removed with additional logic because the reflected waves were of lower amplitude. On longer lines, the reflected waves would actually cause fewer problems for the method because they would be more attenuated. As mentioned earlier, on shorter lines, the reflections could be included in the method, which would reduce the need for multiple measurement devices.

An implemented measurement device would require a sampling frequency of 10 MHz to 100 MHz with support for time synchronization to GPS or synchronization via an optical cable. The input should be compatible with a sensor for voltage or current measurements. Filtering and noise reduction can be performed in the initial signal processing steps to improve signal quality. The real-time processing capabilities for CWT could be implemented in the measurement devices and only the detected local maximum timestamps could be sent to a central location where the rest of the proposed method would be implemented. But as mentioned before, an additional event detection algorithm could be used to detect the presence of

events in the signal. In this case, only a window containing the detected event could be sent to a central location where all steps of the proposed method would be implemented. This would reduce the computational requirements on the measurement devices.

V. CONCLUSION

In this paper, we presented a self-sufficient online method for event localization and characterization of transmission lines. We presented our method in a setup that uses double-sided TW event measurement with an additional measurement device between the end devices. We performed a comprehensive analysis of the capabilities of our method for transmission line characterization. The characterization capabilities of the presented method were tested under various conditions for different line lengths, event types, event locations, and added noise. The specifics of our proposed method were also evaluated with respect to the location of the additional measurement device and synchronization requirements. Based on the results presented in Section IV, we show that the method can be used for transmission line characterization. The characteristic is determined with less than 1% error in most of the experimental setups. We also compared the event localization of our proposed method with another recently developed online method that is not affected by the changing characteristic of the transmission line. Our proposed method improves the event localization in the comparison with other methods and we show that our method can be used in a wider range of applications.

Future work will focus on integrating the proposed method into a test measurement setup and later developing a stand-alone device and system. In addition, we will explore where online transmission line characterization data could be used for new services in addition to improving event localization.

REFERENCES

- [1] F. Wilches-Bernal, A. Bidram, M. J. Reno, J. Hernandez-Alvidrez, P. Barba, B. Reimer, R. Montoya, C. Carr, and O. Lavrova, "A Survey of Traveling Wave Protection Schemes in Electric Power Systems," *IEEE Access*, vol. 9, pp. 72 949–72 969, 2021.
- [2] M. A. Aftab, S. M. S. Hussain, I. Ali, and T. S. Ustun, "Dynamic protection of power systems with high penetration of renewables: A review of the traveling wave based fault location techniques," *International Journal of Electrical Power & Energy Systems*, vol. 114, p. 105410, Jan. 2020.
- [3] X. Liu, A. H. Osman, and O. P. Malik, "Hybrid Traveling Wave/Boundary Protection for Monopolar HVDC Line," *IEEE Transactions on Power Delivery*, vol. 24, no. 2, pp. 569–578, Apr. 2009.
- [4] M. Shafiq, I. Kiiitam, K. Kauhaniemi, P. Taklaja, L. Kütt, and I. Palu, "Performance Comparison of PD Data Acquisition Techniques for Condition Monitoring of Medium Voltage Cables," *Energies*, vol. 13, no. 16, p. 4272, Jan. 2020.
- [5] X. Rao, K. Zhou, Y. Li, G. Zhu, and P. Meng, "A New Cross-Correlation Algorithm Based on Distance for Improving Localization Accuracy of Partial Discharge in Cables Lines," *Energies*, vol. 13, no. 17, p. 4549, Jan. 2020.
- [6] S. Martín Arroyo, M. García-Gracia, and A. Montañés, "The Half-Sine Method: A New Accurate Location Method Based on Wavelet Transform for Transmission-Line Protection from Single-Ended Measurements," *Energies*, vol. 12, no. 17, p. 3293, Jan. 2019.
- [7] F. P. Mohamed, W. H. Siew, J. J. Soraghan, S. M. Strachan, and J. McWilliam, "Partial discharge location in power cables using a double ended method based on time triggering with GPS," *IEEE Transactions on Dielectrics and Electrical Insulation*, vol. 20, no. 6, pp. 2212–2221, Dec. 2013.
- [8] H. Jia, "An Improved Traveling-Wave-Based Fault Location Method with Compensating the Dispersion Effect of Traveling Wave in Wavelet Domain," *Mathematical Problems in Engineering*, vol. 2017, p. e1019591, Feb. 2017.
- [9] R. Liang, Z. Zhang, H. Li, P. Chi, G. Li, and Y. Tao, "Partial discharge location of power cables based on an improved single-terminal method," *Electric Power Systems Research*, vol. 193, p. 107013, Apr. 2021.
- [10] A. Ragusa, P. A. A. F. Wouters, H. G. Sasse, and A. Duffy, "The Effect of the Ring Mains Units for On-Line Partial Discharge Location With Time Reversal in Medium Voltage Networks," *IEEE Access*, vol. 10, pp. 33 844–33 854, 2022.
- [11] M. Mahdipour, A. Akbari, P. Werle, and H. Borsi, "Partial Discharge Localization on Power Cables Using On-Line Transfer Function," *IEEE Transactions on Power Delivery*, vol. 34, no. 4, pp. 1490–1498, Aug. 2019.
- [12] F. Deng, X. Zeng, X. Tang, Z. Li, Y. Zu, and L. Mei, "Travelling-wave-based fault location algorithm for hybrid transmission lines using three-dimensional absolute grey incidence degree," *International Journal of Electrical Power & Energy Systems*, vol. 114, p. 105306, Jan. 2020.
- [13] S. Robson, A. Haddad, and H. Griffiths, "Fault Location on Branched Networks Using a Multiended Approach," *IEEE Transactions on Power Delivery*, vol. 29, no. 4, pp. 1955–1963, Aug. 2014.
- [14] R. Chen, X. Yin, X. Yin, Y. Li, and J. Lin, "Computational Fault Time Difference-Based Fault Location Method for Branched Power Distribution Networks," *IEEE Access*, vol. 7, pp. 181 972–181 982, 2019.
- [15] S. Lin, Z. He, X. Li, and Q. Qian, "Travelling wave time-frequency characteristic-based fault location method for transmission lines," *Generation, Transmission & Distribution, IET*, vol. 6, pp. 764–772, Aug. 2012.
- [16] M. Shafiq, I. Kiiitam, P. Taklaja, L. Kutt, K. Kauhaniemi, and I. Palu, "Identification and Location of PD Defects in Medium voltage Underground Power Cables Using High Frequency Current Transformer," *IEEE Access*, vol. 7, pp. 103 608–103 618, 2019.
- [17] P. Wouters and A. van Deursen, "Thermal Distortion of Signal Propagation Modes Due to Dynamic Loading in Medium-Voltage Cables," *Energies*, vol. 13, no. 17, p. 4436, Jan. 2020.
- [18] Z. Li, J. He, B. Zhang, and Z. Yu, "Influence of frequency characteristics of soil parameters on ground-return transmission line parameters," *Electric Power Systems Research*, vol. 139, pp. 127–132, Oct. 2016.
- [19] A. van Deursen, P. Wouters, and F. Steennis, "Influence of Temperature on Wave Propagation in Low-Voltage Distribution Cables," *IEEE Transactions on Dielectrics and Electrical Insulation*, vol. 28, no. 5, pp. 1785–1792, Oct. 2021.
- [20] M. Kulesh, M. Holschneider, M. S. Diallo, Q. Xie, and F. Scherbaum, "Modeling of Wave Dispersion Using Continuous Wavelet Transforms," *Pure and Applied Geophysics*, vol. 162, no. 5, pp. 843–855, May 2005.
- [21] "Frequency-Dependent Transmission Line - MATLAB & Simulink," <https://www.mathworks.com/help/phymod/sps/ug/frequency-dependent-transmission-line.html>.
- [22] O. Ramos-Leanos, J. L. Naredo, J. Mahseredjian, C. Dufour, J. A. Gutierrez-Robles, and I. Kocar, "A Wideband Line/Cable Model for Real-Time Simulations of Power System Transients," *IEEE Transactions on Power Delivery*, vol. 27, no. 4, pp. 2211–2218, Oct. 2012.
- [23] N. Oussalah, Y. Zebboudj, and S. A. Boggs, "Analytic Solutions for Pulse Propagation in Shielded Power Cable for Symmetric and Asymmetric PD Pulses," *IEEE Transactions on Dielectrics and Electrical Insulation*, vol. 14, no. 5, pp. 1264–1270, Oct. 2007.
- [24] J. Furgal, "Influence of Lightning Current Model on Simulations of Overvoltages in High Voltage Overhead Transmission Systems," *Energies*, vol. 13, no. 2, p. 296, Jan. 2020.